

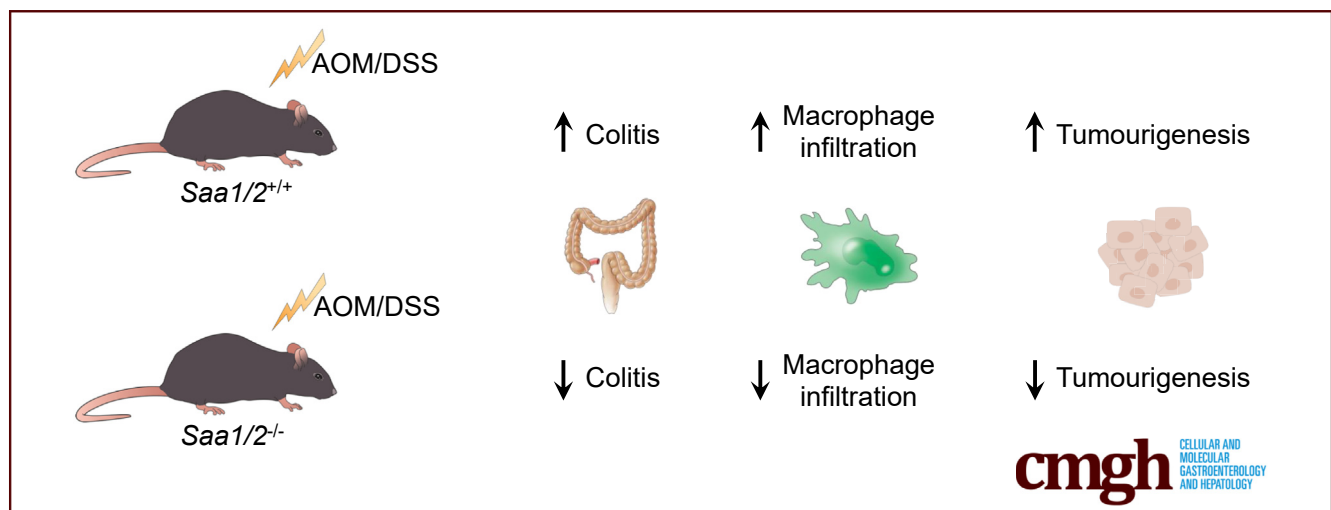
ORIGINAL RESEARCH

Serum Amyloid A Promotes Inflammation-Associated Damage and Tumorigenesis in a Mouse Model of Colitis-Associated Cancer



Tanja A. Davis,¹ Daleen Conradie,¹ Preetha Shridas,² Frederick C. de Beer,² Anna-Mart Engelbrecht,^{1,3} and Willem J. S. de Villiers^{3,4}

¹Department of Physiological Sciences, ³African Cancer Institute, Department of Global Health, ⁴Department of Internal Medicine, Stellenbosch University, Stellenbosch, South Africa; ²Department of Internal Medicine, University of Kentucky, Lexington, Kentucky



SUMMARY

This novel study describes the role of serum amyloid A in a murine model of colitis-associated colon cancer. We show that a lack of serum amyloid A attenuates inflammation-associated colon damage, macrophage infiltration, and tumorigenesis in mice.

BACKGROUND & AIMS: Identifying new approaches to lessen inflammation, as well as the associated malignant consequences, remains crucial to improving the lives and prognosis of patients diagnosed with inflammatory bowel diseases. Although it previously has been suggested as a suitable biomarker for monitoring disease activity in patients diagnosed with Crohn's disease, the role of the acute-phase protein serum amyloid A (SAA) in inflammatory bowel disease remains unclear. In this study, we aimed to assess the role of SAA in colitis-associated cancer.

METHODS: We established a model of colitis-associated cancer in wild-type and SAA double-knockout (*Saa1/2*^{-/-}) mice by following the azoxymethane/dextran sulfate sodium protocol. Disease activity was monitored throughout the study while colon and tumor tissues were harvested for subsequent use in

cytokine analyses, Western blot, and immunohistochemistry +experiments.

RESULTS: We observed attenuated disease activity in mice deficient for *Saa1/2* as evidenced by decreased weight loss, increased stool consistency, decreased rectal bleeding, and decreased colitis-associated tissue damage. Macrophage infiltration, including CD206⁺ M2-like macrophages, also was attenuated in SAA knockout mice, while levels of interleukin 4, interleukin 10, and tumor necrosis factor- α were decreased in the distal colon. Mice deficient for SAA also showed a decreased tumor burden, and tumors were found to have increased apoptotic activity coupled with decreased expression for markers of proliferation.

CONCLUSION: Based on these findings, we conclude that SAA has an active role in inflammatory bowel disease and that it could serve as a therapeutic target aimed at decreasing chronic inflammation and the associated risk of developing colitis-associated cancer. (*Cell Mol Gastroenterol Hepatol* 2021;12:1329–1341; <https://doi.org/10.1016/j.jcmgh.2021.06.016>)

Keywords: Serum Amyloid A; Colitis-Associated Cancer; Inflammation; Macrophage; Colon Cancer.

Chronic relapsing intestinal inflammation and a loss of homeostasis in the gut immune response^{1,2} characterize inflammatory bowel diseases (IBDs), including Crohn's disease and ulcerative colitis. Although IBD significantly impacts a patient's quality of life, the most serious complication is an increased risk of developing colitis-associated cancer (CAC). The importance of mediators that regulate inflammation in the development of IBD and CAC cannot be understated. Accordingly, the identification of such molecules that can be targeted remains a strong focus in the search for effective therapies.³⁻⁵

Serum amyloid A (SAA) is a family of evolutionary conserved proteins implicated in inflammation.^{6,7} SAA1 and SAA2 are prominent acute-phase proteins and systemic levels are up-regulated significantly upon inflammatory or infectious stimuli, peaking 24-48 hours after stimulus before returning to low baseline levels.⁷ Human *SAA3P* is a pseudogene, while SAA4 predominantly is expressed constitutively and thus not considered an acute-phase protein.⁸⁻¹¹ In mice, SAA3 also functions as an acute-phase protein. Functionally, acute-phase SAA (apoSAA, SAA1 and SAA2, including SAA3 in mice) have been reported to chemoattract leukocytes, induce the secretion of various cytokines, and promote angiogenesis and matrix degradation.¹²⁻¹⁶ Unsurprisingly, apoSAA proteins also are implicated in chronic inflammatory states and inflammation-associated pathologies such as diabetes mellitus, Crohn's disease, rheumatoid arthritis, and amyloidosis.^{12,17-19} In addition, several studies also have reported increased apoSAA serum levels and tissue expression in various malignancies, including lung, breast, pancreatic, and colon cancer.²⁰⁻²³ Studies investigating the possibility of a direct role for SAA in cancer have indicated that SAA can promote cancer metastasis, however, such mechanistic studies remain very limited.²⁴⁻²⁸

In the current study, we aimed to identify the role of SAA in CAC by using the well-established azoxymethane/dextran sulfate sodium (AOM/DSS) model in mice lacking both *Saa1* and *Saa2*. We observed that a lack of *Saa1/2* decreases colitis disease activity and associated pathologies. In addition, mice also showed decreased tumorigenesis. Together, these results show that SAA could serve as a therapeutic target in patients diagnosed with IBD to decrease chronic inflammation and the associated risk of developing CAC.

Results

SAA Deficiency Attenuates Colitis Severity

To assess the role of SAA in colitis disease activity, several disease-associated parameters were measured. Although a gradual decrease in relative weight with increased DSS exposure was observed in mice from both genotypes, significantly less weight loss was observed in SAA double-knockout (SAADKO) mice on selected days throughout the model, particularly in cycle 3 of DSS treatment (Figure 1A). Compared with wild-type mice, weight loss in SAADKO mice also was delayed by 2 days in cycle 3 and mice showed improved recovery in cycle 1, while

SAADKO male mice also showed improved recovery in cycle 3 (Figure 1B-D). Disease activity also was assessed by means of the disease activity index (DAI), in which SAADKO mice consistently showed improved scores (Figure 1E-I). With the combined DAI score, a lower score was observed in female SAADKO mice, as well as when the scores of both sexes were combined (Figure 1E). With the individual scores for weight loss (Figure 1F), stool consistency (Figure 1G and H), and rectal bleeding (Figure 1I), lower scores also were observed for SAADKO mice when compared with wild-type mice. However, in each instance, differences were significant for only 1 sex when analyzed separately. The relative colon length of SAADKO male mice also was significantly longer than their wild-type counterparts (Figure 1J). Histomorphologic analyses also were performed on H&E-stained tissue sections of the distal colon to assess the degree of intestinal inflammation (Figure 2). SAADKO mice scored significantly lower than wild-type mice (Figure 2B), in which immune infiltration in both the mucosa and submucosa, as well as extended areas of epithelial defects and loss of architecture in the mucosa, frequently were observed (Figure 2A).

A Deficiency in SAA Alters the Cytokine Profile Within the Distal Colon

To investigate the role of SAA in modulating inflammation in the local environment, we performed a multiplex assay for the cytokines interleukin (IL)4, IL6, IL10, IL17A, and tumor necrosis factor α (TNF- α), with tissue lysates from the distal colon. Compared with wild-type mice, SAADKO mice had decreased levels of IL4, IL10, and TNF- α (Figure 3A). IL6 levels, although also decreased in SAADKO mice, did not differ statistically from those in wild-type mice. The multiplex failed to detect IL17A within the tissue lysates, however, a quantitative real-time polymerase chain reaction (qPCR) experiment with RNA extracted from colon tissue showed no significant differences in *Il17a* expression between wild-type and SAADKO mice (Figure 3B).

SAA Deficiency Decreases Macrophage Infiltration

To assess the degree of macrophage infiltration in the lamina propria of the mucosa and in the submucosa of the distal colon, we performed immunohistochemical staining for the general macrophage marker F4/80. SAADKO mice

Abbreviations used in this paper: AOM, azoxymethane; apoSAA, acute-phase serum amyloid A; CAC, colitis-associated cancer; DAI, disease activity index; DSS, dextran sulfate sodium; IBD, inflammatory bowel disease; IL, interleukin; MCM2, Minichromosome maintenance 2 protein; qPCR, quantitative real-time polymerase chain reaction; SAA, serum amyloid A; SAADKO, serum amyloid A double-knockout; TNF, tumor necrosis factor.

 Most current article

© 2021 The Authors. Published by Elsevier Inc. on behalf of the AGA Institute. This is an open access article under the CC BY-NC-ND license (<http://creativecommons.org/licenses/by-nc-nd/4.0/>).

2352-345X

<https://doi.org/10.1016/j.jcmgh.2021.06.016>

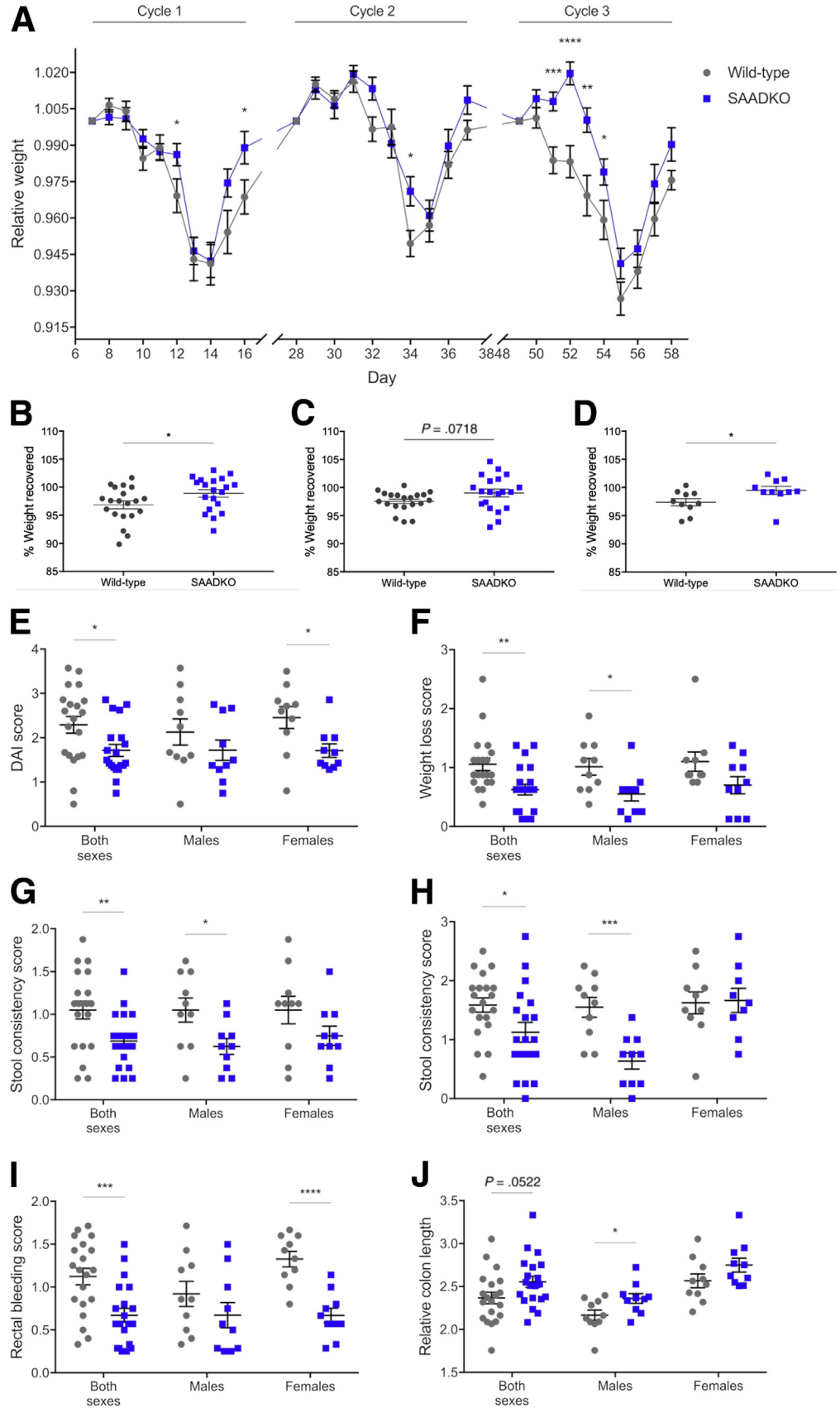


Figure 1. Colitis disease activity is attenuated in serum amyloid A double-knockout (SAADKO) mice. (A) Relative weight of animals during each dextran sulfate sodium (DSS) cycle. Data points include the 5 days of DSS treatment and the first 4 days of the recovery period. Weights are relative to animal weight on day 0 of each cycle. (B) Percentage weight recovered for mice after cycle 1 and (C) cycle 2, as well as for (D) male mice after cycle 3. Weight recovery was calculated as the percentage animal weight on day 4 of the recovery period relative to the weight at the start of the DSS cycle. (E) Average disease activity score (DAI) score of animals during DSS cycle 1. (F) Average weight loss score of animals during DSS cycle 3. (G) Average stool consistency score of animals during cycle 1 and (H) cycle 3. (I) Average rectal bleeding score of animals during DSS cycle 1. (J) Relative colon length of animals. Measurements are relative to the last weight measurement of each animal. * $P < .05$, ** $P < .01$, *** $P < .001$, and **** $P < .0001$.



Figure 2. Colitis-associated histomorphologic abnormalities are decreased in serum amyloid A double-knockout (SAADKO) mice. (A) Representative images of H&E stains of the distal colon of wild-type and SAADKO mice. Epithelial defects and loss of architecture in the mucosa are highlighted (*solid arrow*), as well as immune infiltrates in the mucosa (*dashed arrow*) and submucosa (*dotted arrow*). (B) Quantified histomorphological scores for wild-type and SAADKO mice. ****P < .01.**

showed significantly less macrophage infiltration in the distal colon when compared with wild-type mice (Figure 4). Although M1-like inducible nitric oxide synthase-positive (iNOS⁺) macrophages were abundant, no differences in the amount of these macrophages were observed between SAADKO and wild-type mice. In contrast, although M2-like macrophages staining positive for CD206 were less abundant, the distal colon of SAADKO mice had significantly less CD206⁺ macrophages when compared with wild-type mice.

SAA Deficiency Decreases Tumorigenesis

To determine whether the effects of SAA include a role in tumorigenesis, we compared the tumor characteristics between the 2 genotypes. SAADKO mice had significantly fewer tumors than their wild-type counterparts (Figure 5A). The majority of the tumors observed in the distal colon of the mice ranged between 1 and 2 mm in size, and SAADKO mice showed a significant decrease in these tumor occurrences (Figure 5B). We also performed Western blot experiments with the isolated tumors. In general, tumors isolated from SAADKO mice showed a lesser proliferative phenotype than tumors isolated from wild-type mice. Increased expression of the proliferation marker Minichromosome maintenance 2 protein (MCM2) was detected in tumors from wild-type mice (Figure 5C and D). This coincided with decreased levels of apoptosis, as evidenced by a decrease in the cleaved (active) form of the apoptosis marker, caspase 3 (Figure 5C and F). We also assessed whether there were differences in the level of β -catenin. Indeed, tumors from wild-type mice showed increased levels of active β -catenin, although, interestingly, tumors from female wild-type mice showed levels similar to those of SAADKO mice (Figure 5C and E). Intratumor IL6 expression also was assessed, but no differences were observed (Figure 5C). To further support these results, we performed immunohistochemical staining of Ki-67 and determined its expression in areas of dysplasia within the distal colon. In agreement with the previous results, decreased Ki-67 staining intensity was

observed in SAADKO mice when compared with wild-type mice (Figure 6).

Deficiency in *Saa1* and *Saa2* Limits *Saa3* Expression

To determine whether the lack of *Saa1* and *Saa2* affects *Saa3* expression in mice, we performed qPCR to quantify *Saa3* gene expression in the tumors and distal colons of mice. In both tissues, we detected a significant decrease in *Saa3* gene expression in SAADKO mice when compared with wild-type mice (Figure 7).

Discussion

SAA is a major acute-phase protein and its persistent activation is widely associated with inflammation-associated pathologies, including ulcerative colitis and Crohn's disease.^{18,29,30} In IL2^{-/-} and IL10^{-/-} mouse models of colitis, serum SAA levels were reported to increase with animal age and correlate with disease severity.³¹⁻³³ In this study we investigated the role of SAA in a mouse model of CAC by comparing wild-type mice and mutant mice lacking *Saa1/2*. The AOM/DSS model is widely used to study CAC in rodents because of its simplicity, reproducibility, and ability to recapitulate the events that promote colorectal carcinogenesis related to chronic inflammation in human beings.³⁴ Key features of colitis that often are assessed in this and other models of colitis include macroscopic assessments such as animal weight and the DAI, as well as microscopic features such as mucosal damage, immune cell infiltrates, and cytokine levels.

In our model, mice lacking *Saa1/2* showed attenuated colitis disease activity when compared with their wild-type counterparts. SAADKO mice showed reduced weight loss (Figure 1A), improved recovery (Figure 1B-D), lower DAI scores (Figure 1E-I), and lessened histologic damage (Figure 2). These results are in agreement with recent findings from Lee et al,³⁵ in which mice deficient for *Saa1-3* showed reduced colitis-associated histologic features, and mice lacking *Saa1/2* showed attenuated and delayed disease

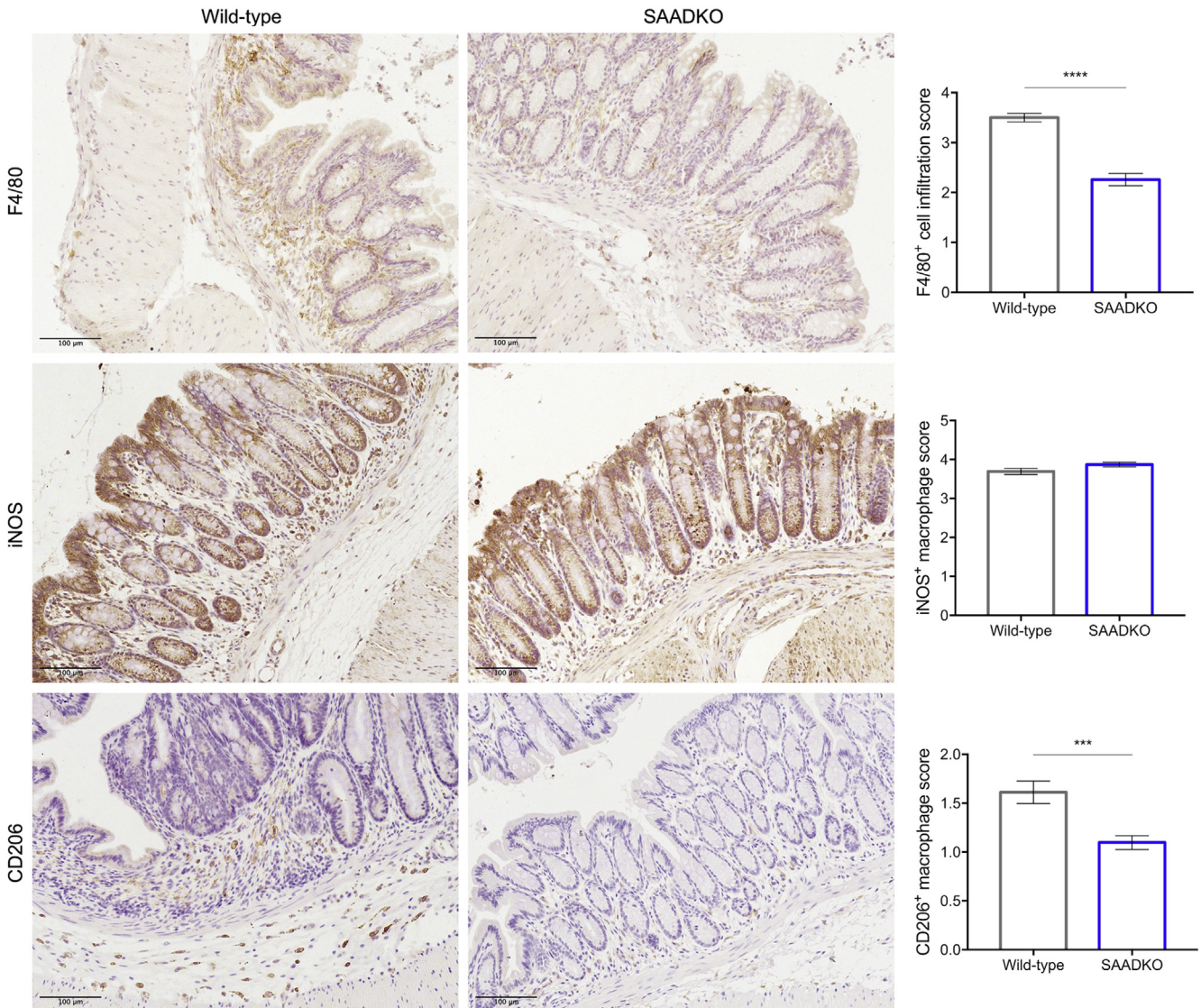


Figure 3. Macrophage infiltration is decreased in serum amyloid A double-knockout (SAADKO) mice. Representative immunohistochemical images of the distal colon of wild-type and SAADKO mice stained with antibodies for F4/80, inducible nitric oxide synthase (iNOS), and CD206, and hematoxylin as counterstain, along with quantified scoring results for each marker. *** $P < .001$ and **** $P < .0001$.

onset in a model of experimental autoimmune encephalomyelitis. In these models, SAA1 was found to promote pathogenic T-helper 17 cell responses, including a gene signature consisting of several chronic inflammatory disease-associated genes.

Immune cells play a central role in inflammation and extensive immune cell infiltration represents a hallmark of colitis. To determine whether SAA influenced the infiltration of macrophages, we assessed their presence in the lamina propria of the distal colon. SAADKO mice showed a decreased number of macrophages when compared with wild-type mice (Figure 4). SAA also has been reported previously to function as a chemokine for various immune cells, including monocytes,^{13,36} and thus the absence of SAA1/2 in the lamina propria of SAADKO mice also could

have contributed directly to reduced macrophage infiltration. Interestingly, although we did not observe any changes in the number of macrophages staining positive for iNOS, representative of classic proinflammatory M1-like macrophages, we did observe a significant reduction in CD206⁺ M2 macrophages, which represents M2-like macrophages. This is supported by recent findings from Sun et al,³⁷ who showed that SAA induced several M2-macrophage markers, including CD206, in both human blood-derived monocytes and murine bone marrow-derived and peritoneal-derived macrophages. Furthermore, SAA-activated macrophages also showed enhanced efferocytosis of apoptotic neutrophils, a classic function of M2 macrophages during tissue repair and remodeling. Work by Wang et al³⁸ also described the M2b-like activation of murine bone marrow-derived

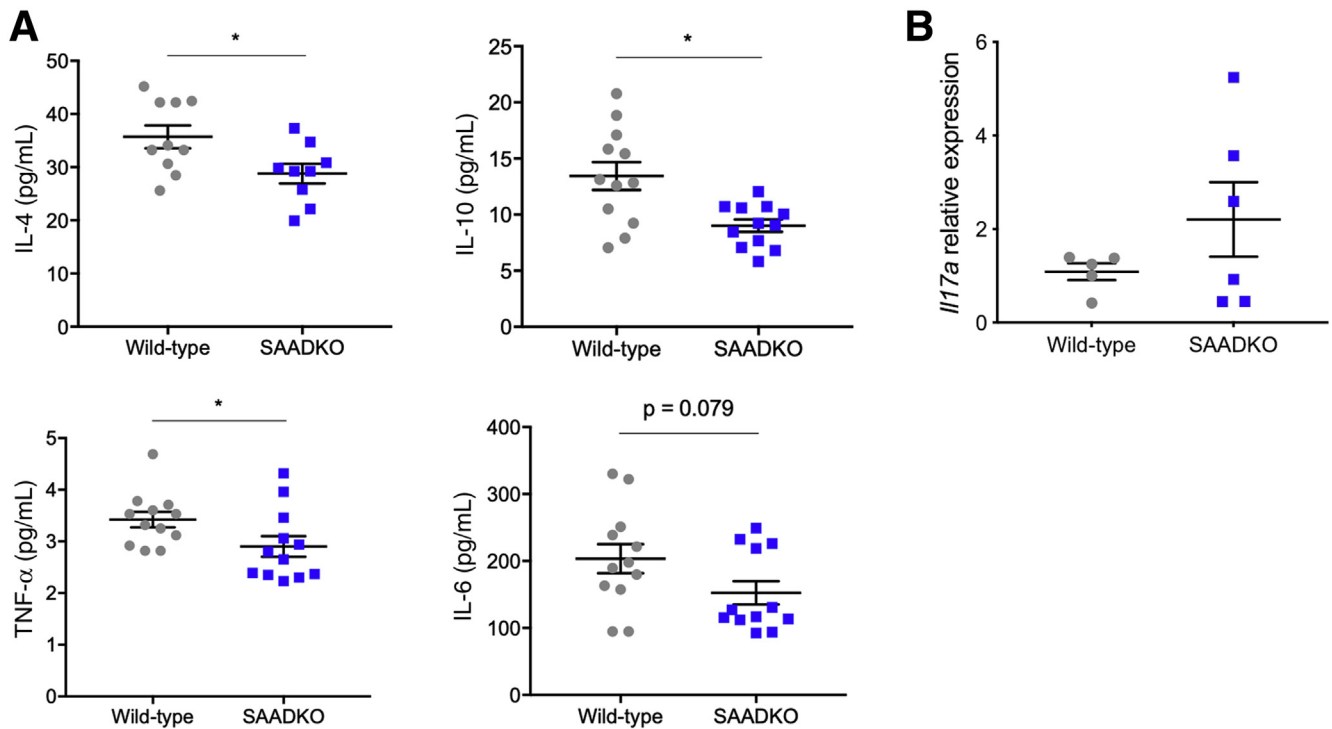


Figure 4. Cytokine profiles are altered in serum amyloid A double-knockout (SAADKO) mice. (A) Concentrations of interleukin (IL)4, IL10, tumor necrosis factor α (TNF- α), and IL6 in the distal colon of wild-type and SAADKO mice, as determined with a multiplex assay. (B) Relative gene expression of *Il17a* in the distal colon of wild-type and SAADKO mice. * $P < .05$.

macrophages after exposure to recombinant SAA, however, the expression of CD206 was not assessed.

Several in vitro studies have reported SAA-mediated cytokine production in various cell types.^{14,38,39} In particular, TNF- α and IL6 cytokines play vital roles in colitis and CAC.⁴⁰ To determine whether SAA1/2 mediated cytokine alterations in vivo, we assessed the local concentrations of these and other cytokines in the distal colon after acute colitis. As expected, SAADKO mice showed decreased levels of the proinflammatory cytokines TNF- α and IL6, although the latter did not reach statistical significance (Figure 3A). A significant decrease in IL4 and IL10 also was observed. SAA has been shown previously to induce IL10 expression, as part of the M2b-like activation of macrophages.³⁸ Of note, this subcategory of alternatively activated macrophages also secrete TNF- α and IL6, and these cytokines also were induced by SAA during macrophage activation.

Numerous studies have reported on serum and tissue SAA expression levels in various malignancies, including colon cancer, in which increased SAA generally is correlated with more advanced disease and poor survival.^{20,21,23,41} Mechanistic studies investigating a direct role for SAA in tumorigenesis, however, are limited. In our model of CAC, mice lacking *Saa1/2* showed a decreased tumor burden when compared with wild-type mice (Figure 5A and B). Furthermore, when compared with those of SAADKO mice, tumors in wild-type mice also were more proliferative, as evidenced by increased MCM2 (Figure 5C and D) and Ki-67 (Figure 6) expression, as well as decreased levels of apoptosis, as evidenced by decreased caspase 3 activation

(Figure 5C and F). Expression of active β -catenin, which frequently shows aberrant activation in colon cancer, also was increased in tumors from wild-type mice (Figure 5C and E). The majority of studies describing a role for SAA in cancer relates to tumor metastasis, however, recombinant SAA was reported to increase the proliferation of glioma cells in vitro.²⁶ In light of the important role that inflammation plays in tumorigenesis in CAC, it also should be considered that the decreased tumor burden observed in SAADKO mice may be owing to the attenuated inflammation and colitis disease activity in these mice. In addition, the role of macrophages themselves also should not be overlooked. Depletion of macrophages was shown to reduce the tumor burden of mice in an AOM/DSS model.⁴² Here, decreased levels of the cytokines IL10 and IL6 also were observed in the distal colons of mice.

Human apoSAA consists only of SAA1 and SAA2, with SAA3 being a pseudogene. Mice, however, have a functional Saa3 protein, which has been reported to function in inflammation.^{35,43} Ebert et al⁴⁴ reported that SAA can modulate its own expression, and we previously observed that treatment of Phorbol myristate acetate (PMA)-differentiated human monocytic cell line (THP-1) monocytes with recombinant SAA1 induces SAA1 expression (data not shown), therefore, we investigated whether a lack of *Saa1/2* affected *Saa3* expression in our model of CAC. Indeed, decreased *Saa3* expression was detected in both the distal colon and colonic tumors of SAADKO mice (Figure 7). We hypothesize that 3 potential scenarios could contribute to these results. First, that the lack of *Saa1/2* signaling in

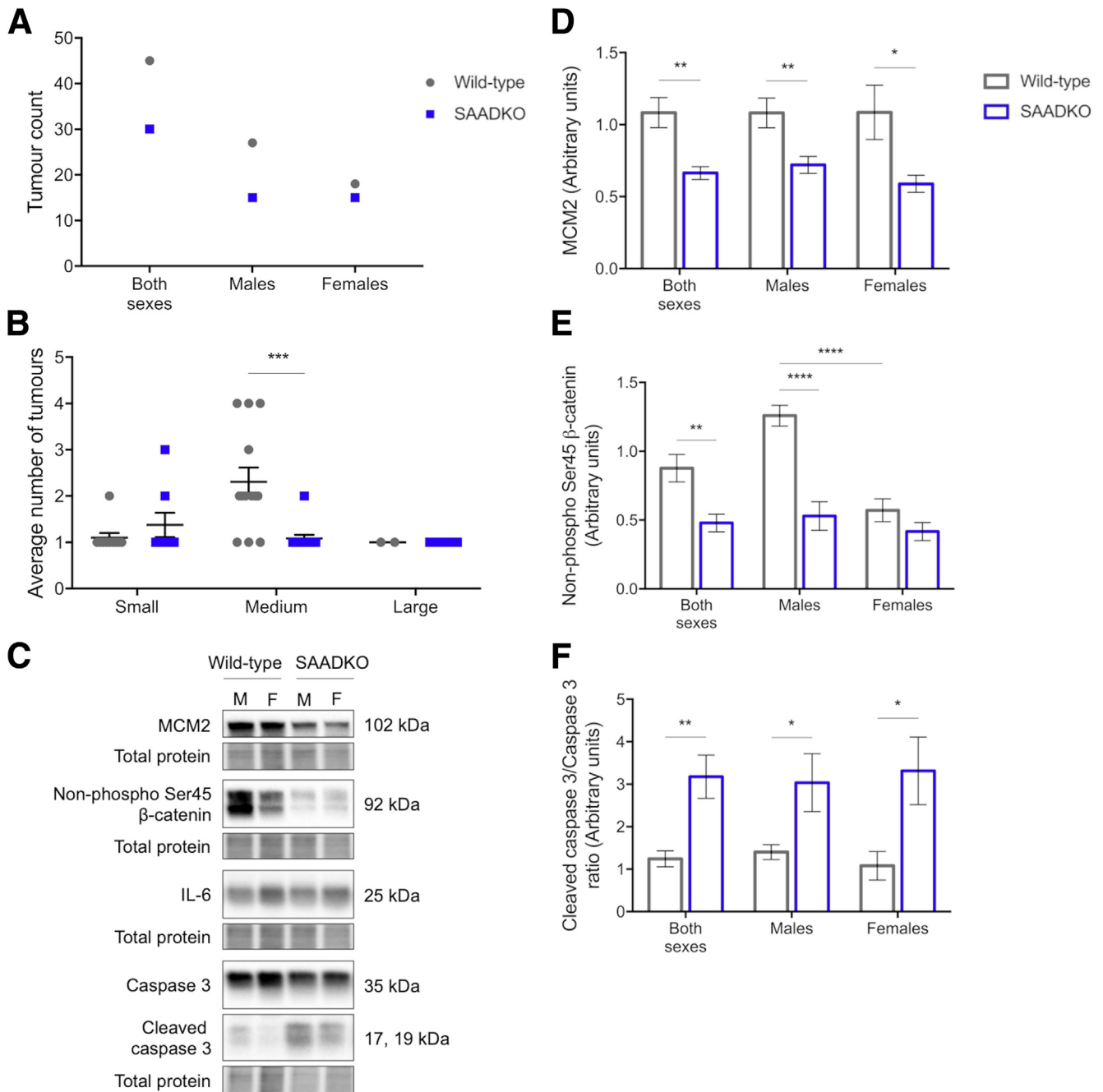


Figure 5. Tumorigenesis is decreased in serum amyloid A double-knockout (SAADKO) mice. (A) Total amount of tumors recorded in mice. (B) Average number of tumors in mice, according to size, where small is less than 1 mm, medium is 1–2 mm, and large is greater than 2 mm. These sizes, respectively, represent 25%, 70%, and 5% of tumors in wild-type mice, and 39%, 47%, and 14% of tumors in SAADKO mice. (C) Representative images of Western blots, along with quantified results for (D) MCM2, (E) non-phospho Ser45 (active) β-catenin, and (F) the ratio of cleaved caspase 3 over total caspase 3. * $P < .05$, ** $P < .01$, *** $P < .001$, and **** $P < .0001$.

SAADKO resulted in reduced *Saa3* expression. Although it previously has been shown that recombinant Saa1 can induce *Saa3* gene expression,²⁴ the precise signaling mechanism(s) is unclear. SAA can bind various cell surface receptors, and reporter assays performed in cells lacking these receptors could be performed to delineate the feedback loop involving Saa1/2 and Saa3. Second, *Saa3* expression could be

decreased owing to the attenuated inflammation in these mice. Third, because macrophages are reported to be a major local source of Saa3³² and we observed decreased macrophage infiltration in the distal colon, the reduction in *Saa3* expression also could be attributed to a decrease in the cells responsible for its secretion. Indeed, basal expression of *Saa3* was found to be significantly higher in macrophages than in

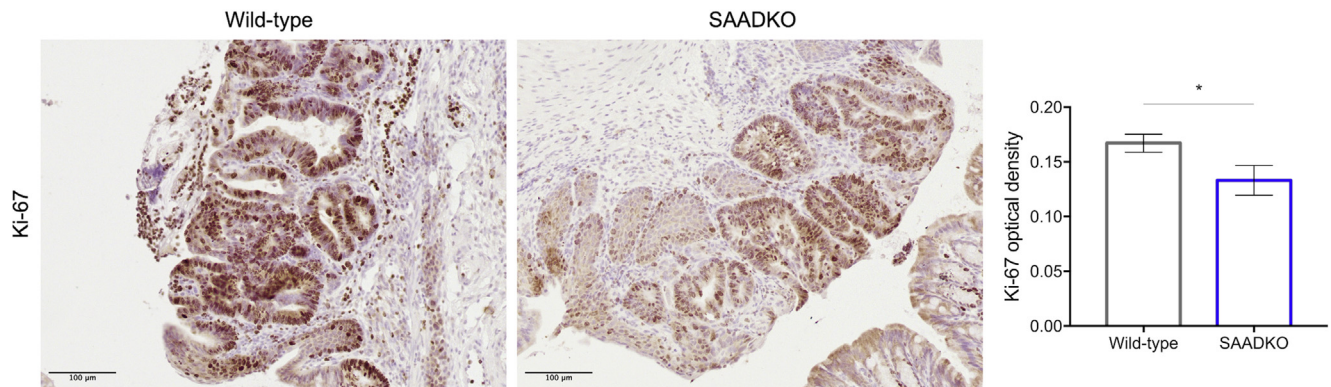


Figure 6. Ki-67 expression is decreased in serum amyloid A double-knockout (SAADKO) mice. Representative immunohistochemical images of areas of dysplasia in the distal colon of wild-type and SAADKO mice stained with Ki-67, along with the quantified intensity. $^*P < .05$.

colon epithelial cells,⁴⁵ suggesting that a small decrease in the number of macrophages could have a large impact on the level of expression.

In our model, we observed a number of sex-based differences in the results. This includes the assessments of colitis disease activity (Figure 1B–G) as well as differential expression of β -catenin between males and females in the tumors of mice (Figure 5C and E). Although the majority of the colitis disease activity assessments showed the same trend between males and females, albeit nonsignificantly in the latter, the potential influence of sex hormones should not be overlooked. Indeed, sex-based differences in colitis murine models have been observed before, and the incidence of IBD among men and women also differs.^{46–48} Furthermore, sex-based differences in immune response and the risk for several autoimmune diseases have been well described.⁴⁹ It is hypothesized that female sex hormones provide a protective effect owing to anti-inflammatory properties, however proinflammatory and anti-inflammatory effects were reported in 2 different models of murine colitis, indicating that these properties may be dependent on the type of model.⁵⁰

In a recent study, increased SAA expression was detected and associated with an aggravated

neuroinflammatory response in male mice compared with females after traumatic brain injury.⁵¹ This could suggest that differences in inflammatory-based diseases between wild-type and SAA knockout mice, such as in this study, could be more evident in males, although this would require further investigation.

Collectively, our results show that the presence of SAA aggravates colitis disease severity and promotes tumorigenesis in a mouse model of CAC. Our findings are consistent with several other reports describing a pathologic role for SAA in inflammation-associated diseases.^{35,51–53} Traditionally, SAA is described as a proinflammatory mediator of the acute-phase response. This description is fitting given its association with inflammatory disease and the reported proinflammatory functions therein. However, alternative functions relating to the activation of M2 macrophages suggest a potential role in the resolution of inflammation, immunoregulation, and wound healing. Some of our reported results also support this. Nevertheless, the function of SAA most likely is influenced by the nature of the inflammatory episode and the relevant constituents. Indeed, SAA was reported to modulate fibrogenic responses in the liver in either a positive or negative fashion, depending on the presence of nuclear factor- $\kappa\beta$.⁵⁴ Deciphering the true

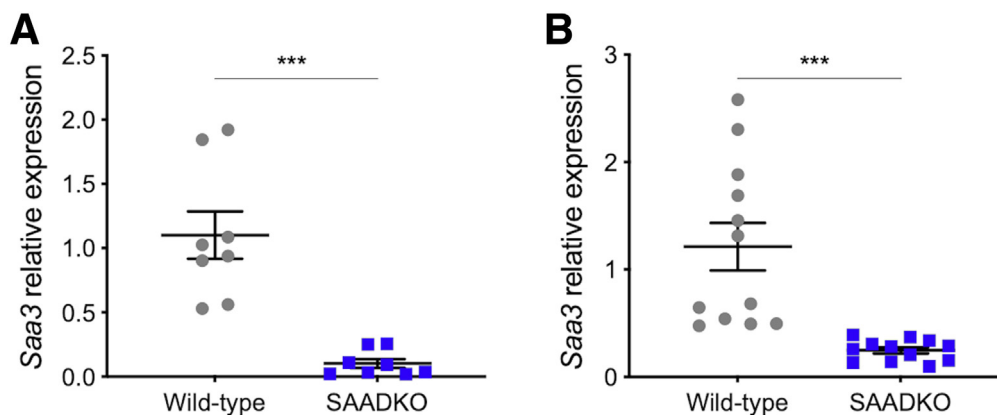


Figure 7. Saa3 expression is decreased in serum amyloid A double-knockout (SAADKO) mice. Saa3 gene expression (A) within tumors and (B) in the distal colons of wild-type and SAADKO mice. $***P < .001$.

nature and impact of SAA modulation represents an exciting new avenue for research and should be the focus of future research. Ultimately, this holds the potential of fine-tuning the inflammatory process with the end goal of improving patient quality of life and prognosis.

Materials and Methods

Animal Models

Ethical clearance was obtained from the Stellenbosch University Research Ethics Committee (ACU-2019-6307) and all procedures were performed under the committee's guidelines. Ten male and 10 female SAADKO (*Saa1*^{-/-} *Saa2*^{-/-}) mice,⁵⁵ 8 weeks old, were used in the study along with 20 age- and sex-matched wild-type C57BL/6 control mice. All mice were housed at the Stellenbosch University animal facility in individually ventilated cages with autoclaved bedding and standard chow and water provided ad libitum.

CAC was induced by following the AOM/DSS protocol, modified from Thaker et al.⁵⁶ Briefly, mice received an intraperitoneal injection of 12.5 mg/kg AOM (Sigma-Aldrich, St. Louis, MO), prepared in saline. One week later, DSS (40 kilodaltons; Alfa Aesar, Ward Hill, MA) treatment commenced and was administered in autoclaved drinking water at a concentration of 2.5% for a total of 5 days, followed by a recovery period of 16 days. DSS treatment was administered for a total of 3 cycles. Animals were monitored daily, and weight measurements and stool samples were collected every day during DSS treatment as well as the first 4 days of the recovery period. At the end of the third DSS cycle, mice were killed and samples were collected. For colon length measurements, images were taken of the excised colon and the length was measured from the cecocolic junction to the rectum on scaled images with Fiji (Madison, WI) software.⁵⁷

Scoring for the DAI was based on the literature^{58,59} and was calculated as the sum of individual scores for weight loss (0 = 0%; 1 = 0%–4.99%; 2 = 5%–9.99%; 3 = 10%–14.99%; and 4 = 15%–20%), stool consistency (0 = normal stool; 2 = loose/pasty stool; 3 = delayed defecation; and 4 = diarrhea), and rectal bleeding (0 = negative; 2 = positive for occult blood; and 4 = gross rectal bleeding). The presence of fecal occult blood was detected by dissolving the pellet in dH₂O and mixing a sample of the supernatant with a luminol-based solution.⁶⁰

For colon tissue samples used in multiplex analyses, an acute-colitis model was established with 8-week-old, sex-matched, wild-type and SAADKO mice (N = 12 per genotype). Mice received 2.5% DSS, administered for a total of 5 days in autoclaved drinking water, before death and sample collection.

Histology, Immunohistochemistry, and Image Analyses

Colon tissues were rolled using the Swiss-roll method before being formalin-fixed and wax-embedded. Tissue sections were cut to 5 μ m. Standard H&E staining was performed to assess tissue morphology. For immunohistochemistry, sections underwent deparaffinization and

rehydration before heat-mediated antigen retrieval in sodium citrate buffer (with the exception of sections stained for F4/80, which underwent antigen retrieval in Tris-EDTA buffer). Sections were blocked in 5% goat serum for 90 minutes before overnight primary antibody incubation. The following primary antibodies were used: F4/80 (MA516363; Thermo Fisher Scientific, Waltham, MA) as a general marker for macrophages, iNOS (PA1036; Thermo Fisher Scientific) to identify M1-like macrophages, CD206 (NBP1-90020; Novus Bio, Centennial, CO) to identify M2-like macrophages, and Ki-67 (SP6) (ab16667; Abcam, Cambridge, UK), used as a marker of proliferation. On the following day, sections were blocked in 3% hydrogen peroxide for 10 minutes and incubated in goat anti-rabbit secondary (7074; Cell Signaling Technology, Danvers, MA) for 45 minutes. Sections were developed with 3,3'-diaminobenzidine tetra hydrochloride chromogen (ab64238; Abcam) for 10 minutes and counterstained with hematoxylin before dehydration and mounting. Brightfield images were acquired on a Nikon Eclipse E400 microscope (Tokyo, Japan) equipped with a DS-Fi2 color digital camera and the same acquisition settings were maintained throughout imaging of all sections for each stain. At least 3 different areas of the distal colon from a total of 20 animals were imaged using a 20 \times objective, with equal representation of genotype and sex.

Histomorphologic evaluation of intestinal inflammation was calculated as the sum of 2 parameters,⁶¹ and was scored as follows: inflammatory infiltration (0 = absent; 1 = mild, limited to mucosa; 2 = moderate, including mucosa and submucosa; and 3 = marked, extended transmural) and epithelial and mucosal architecture (0 = normal; 1 = focal erosion; 2 = erosion \pm focal ulceration; and 3 = extended ulceration \pm granulation tissue). Macrophage infiltration was defined as the degree of F4/80⁺ cell infiltration in the lamina propria of the mucosa and in the submucosa, according to the following scores: 0 = absent; 1 = minimal; 2 = moderate; 3 = abundant; and 4 = extensive. The amount of iNOS and CD206-positive macrophages was determined by assessing the relative percentage of cells positive for F4/80 and either iNOS or CD206 in corresponding areas of individually stained consecutive sections. To aid in the identification of positive cells, color deconvolution was performed with the CMYK color model⁶² using Fiji software. The relative percentages of iNOS⁺/F4/80⁺ and CD206⁺/F4/80⁺ cells were scored as follows: 0 = 0%; 1 = 1%–25%; 2 = 26%–50%; 3 = 51%–75%; and 4 = 76%–100%. Ki-67 expression in areas of dysplasia was assessed by quantifying the optical density of the 3,3'-diaminobenzidine tetra hydrochloride chromogen after color deconvolution with the built-in HDAB vector in Fiji and using the following equation: optical density, OD = log (maximum intensity/mean intensity).^{63,64}

Western Blot

Colonic tumors were snap-frozen in liquid nitrogen after harvest and stored at -80°C until further processing. Tumors were cut into pieces, followed by incubation and sonication in RIPA buffer supplemented with a protease inhibitor cocktail (Roche, Basel Switzerland). Protein

concentration was determined with a standard Bradford assay and samples were mixed with Laemli's sample buffer before electrophoresis. Protein samples were separated on 12% TGX FastCast gels (Bio-Rad, Hercules, CA), transferred onto polyvinylidene difluoride membranes (Bio-Rad), and blocked in 5% milk for 60 minutes before overnight primary antibody incubation. The following primary antibodies were used: MCM2 (ab108935; Abcam), caspase 3 (9662; Cell Signaling Technology), non-phospho (Ser45) β -catenin (19807; Cell Signaling Technology), and IL6 (ab9324; Abcam).

On the following day, membranes were incubated in anti-rabbit secondary antibody (7074; Cell Signaling Technology) for 60 minutes before developing with Clarity ECL (Bio-Rad).

Analyses were performed with Image Lab software (Bio-Rad), using the total protein content on each membrane for normalization and a total of 8 animals per genotype.

qPCR

Tissues were placed in RNAlater (Sigma-Aldrich) immediately after harvest and subsequently stored at -80°C before RNA extraction. Tissues were cut into smaller pieces and the RNA was extracted with TRIzol Reagent (Thermo Fisher Scientific) according to the manufacturer's protocol. Total RNA was incubated with DNase I (ThermoFisher Scientific) before being reverse-transcribed with the Luna-Script RT mix (New England Biolabs, Ipswich, MA). Complementary DNA (5 ng) was used as a template for qPCR reactions performed with the Luna Universal qPCR Master Mix (New England Biolabs) on a StepOnePlus instrument (Applied Biosystems, Waltham, MA). The following primers were used for amplification: *Saa3* (NM_011315.3) forward: 5'-ACAGCCAAAGATGGGTCCAG-3', reverse: 5'-CTGGCATCGTGACTTT-3' (amplicon length, 190 bp); *Il-17a* (NM_010552.3) forward: 5'-GGACTCTCCACCGCAATGAA-3', reverse: 5'-TTTCCCTCCGATTTGACACA-3' (amplicon length, 94 bp); *Eef2* (NM_007907.2) forward: 5'-AGTGTCTGAGCAAGTGGTG-3', reverse: 5'-CGGTGAAGCAAAGGACTCA-3' (amplicon length, 144 bp); and *Tbp* (NM_013684.3) forward: 5'-GCAGTGCCAGCATCACTAT-3', reverse: 5'-GCCCTGAGCATAAGGTGGAA-3' (amplicon length, 160 bp). All primers were designed to span exon-exon boundaries. The quantitation cycle values of *Saa3* and *Il17a* were normalized to the values of the *Eef2* and *Tbp* reference genes, and gene expression was quantified using the delta-delta quantitation cycle method. Results are shown as expression relative to wild-type samples (N = 4–6).

Multiplex Cytokine Analyses

Concentrations of TNF- α , IL6, IL17A, IL4, and IL10 were determined in colon tissue lysate samples by means of multiplex analyses using a premixed mouse Magnetic Luminex Assay (R&D Systems, Minneapolis, MN), performed according to the manufacturer's guidelines, on a Bioplex 200 Luminex instrument and using Bioplex Manager software version 6.1. To prepare the lysates, the distal end of the colon (12–20 mm) was cleaned before being placed in

sterile phosphate-buffered saline containing a protease inhibitor cocktail (Roche). The tissue then was homogenized, and an equal volume of Cell Lysis Buffer 2 (R&D Systems) was added and the tissues were lysed for 30 minutes at room temperature with gentle agitation. Cellular debris were removed by centrifugation at $16,000 \times g$ for 20 minutes at 4°C . Aliquots were prepared and stored at -80°C until assayed. Concentrations of the cytokines were normalized according to tissue length (N = 6).

Statistical Analyses

All data are shown as means \pm SEM. Data were assessed for normality with the Shapiro-Wilk normality test and statistical significance was assessed with either an unpaired Student *t* test or the Mann-Whitney *U* test, using $P < .05$ as the cut-off value for significant differences. All analyses were performed with GraphPad Prism version 7 (San Diego, CA).

References

- Francescone R, Hou V, Grivennikov SI. Cytokines, IBD, and colitis-associated cancer. *Inflamm Bowel Dis* 2015; 21:409–418.
- Asquith M, Powrie F. An innately dangerous balancing act: intestinal homeostasis, inflammation, and colitis-associated cancer. *J Exp Medicine* 2010;207:1573–1577.
- Porter RJ, Andrews C, Brice DP, Durum SK, McLean MH. Can we target endogenous anti-inflammatory responses as a therapeutic strategy for inflammatory bowel disease? *Inflamm Bowel Dis* 2018;24:2123–2134.
- Neurath MF. New targets for mucosal healing and therapy in inflammatory bowel diseases. *Mucosal Immunol* 2014;7:6–19.
- Wang D, DuBois RN. The role of COX-2 in intestinal inflammation and colorectal cancer. *Oncogene* 2010; 29:781–788.
- Sack GH. Serum amyloid A - a review. *Mol Med* 2018; 24:46.
- Zhang Y, Zhang J, Sheng H, Li H, Wang R. Acute phase reactant serum amyloid A in inflammation and other diseases. *Adv Clin Chem* 2019;90:25–80.
- Kluve-Beckerman B, Drumm ML, Benson MD. Non-expression of the human serum amyloid A three (SAA3) gene. *DNA Cell Biol* 1991;10:651–661.
- Buck M, Gouwy M, Wang J, Snick J, Opendakker G, Struyf S, Damme J. Structure and expression of different serum amyloid A (SAA) variants and their concentration-dependent functions during host insults. *Curr Med Chem* 2016;23:1725–1755.
- Jumeau C, Awad F, Assrawi E, Cobret L, Duquesnoy P, Giurgea I, Valeyre D, Grateau G, Amselem S, Bernaudin J-F, Karabina S-A. Expression of SAA1, SAA2 and SAA4 genes in human primary monocytes and monocyte-derived macrophages. *PLoS One* 2019;14:e0217005.
- Whitehead AS, de Beer MC, Steel DM, Rits M, Lelias JM, Lane WS, de Beer FC. Identification of novel members of the serum amyloid A protein superfamily as constitutive apolipoproteins of high density lipoprotein. *J Biol Chem* 1992;267:3862–3867.

12. Mullan RH, Bresnihan B, Golden-Mason L, Markham T, O'Hara R, FitzGerald O, Veale DJ, Fearon U. Acute-phase serum amyloid A stimulation of angiogenesis, leukocyte recruitment, and matrix degradation in rheumatoid arthritis through an NF- κ B-dependent signal transduction pathway. *Arthritis Rheum* 2006;54:105–114.
13. Badolato R, Wang JM, Murphy WJ, Lloyd AR, Michiel DF, Bausserman LL, Kelvin DJ, Oppenheim JJ. Serum amyloid A is a chemoattractant: induction of migration, adhesion, and tissue infiltration of monocytes and polymorphonuclear leukocytes. *J Exp Med* 1994; 180:203–209.
14. Furlaneto CJ, Campa A. A novel function of serum amyloid A: a potent stimulus for the release of tumor necrosis factor- α , interleukin-1 β , and interleukin-8 by human blood neutrophil. *Biochem Biophys Res Commun* 2000;268:405–408.
15. Connolly M, Rooney PR, McGarry T, Maratha AX, McCormick J, Miggin SM, Veale DJ, Fearon U. Acute serum amyloid A is an endogenous TLR2 ligand that mediates inflammatory and angiogenic mechanisms. *Ann Rheum Dis* 2016;75:1392.
16. Seidl SE, Pessolano LG, Bishop CA, Best M, Rich CB, Stone PJ, Schreiber BM. Toll-like receptor 2 activation and serum amyloid A regulate smooth muscle cell extracellular matrix. *PLoS One* 2017;12:e0171711.
17. Marzi C, Huth C, Herder C, Baumert J, Thorand B, Rathmann W, Meisinger C, Wichmann H-E, Roden M, Peters A, Grallert H, Koenig W, Illig T. Acute-phase serum amyloid A protein and its implication in the development of type 2 diabetes in the KORA S4/F4 study. *Diabetes Care* 2013;36:1321–1326.
18. Yarur AJ, Quintero MA, Jain A, Czul F, Barkin JS, Abreu MT. Serum amyloid A as a surrogate marker for mucosal and histologic inflammation in patients with Crohn's disease. *Inflamm Bowel Dis* 2017;23:158–164.
19. Jayaraman S, Gantz DL, Haupt C, Gursky O. Serum amyloid A forms stable oligomers that disrupt vesicles at lysosomal pH and contribute to the pathogenesis of reactive amyloidosis. *Proc Natl Acad Sci U S A* 2017; 114:E6507–E6515.
20. Cho WCS, Yip TT, Cheng WW, Au JSK. Serum amyloid A is elevated in the serum of lung cancer patients with poor prognosis. *Br J Cancer* 2010;102:1731–1735.
21. Yang M, Liu F, Higuchi K, Sawashita J, Fu X, Zhang L, Zhang L, Fu L, Tong Z, Higuchi K. Serum amyloid A expression in the breast cancer tissue is associated with poor prognosis. *Oncotarget* 2016;7:35843–35852.
22. Djurec M, Graña O, Lee A, Troulé K, Espinet E, Cabras L, Navas C, Blasco MT, Martín-Díaz L, Burdiel M, Li J, Liu Z, Vallespinós M, Sanchez-Bueno F, Sprick MR, Trumpp A, Sainz B, Al-Shahrour F, Rabadan R, Guerra C, Barbacid M. Saa3 is a key mediator of the protumorigenic properties of cancer-associated fibroblasts in pancreatic tumors. *Proc Natl Acad Sci U S A* 2018;115:201717802.
23. Gutfeld O, Prus D, Ackerman Z, Dishon S, Linke RP, Levin M, Urieli-Shoval S. Expression of serum amyloid A, in normal, dysplastic, and neoplastic human colonic mucosa: implication for a role in colonic tumorigenesis. *J Histochem Cytochem* 2005;54:63–73.
24. Hansen MT, Forst B, Cremers N, Quagliata L, Ambartsumian N, Grum-Schwensen B, Klingelhöfer J, Abdul-AI A, Herrmann P, Osterland M, Stein U, Nielsen GH, Scherer PE, Lukanidin E, Sleeman JP, Grigorian M. A link between inflammation and metastasis: serum amyloid A1 and A3 induce metastasis, and are targets of metastasis-inducing S100A4. *Oncogene* 2015;34:424–435.
25. Lee JW, Stone ML, Porrett PM, Thomas SK, Komar CA, Li JH, Delman D, Graham K, Gladney WL, Hua X, Black TA, Chien AL, Majmundar KS, Thompson JC, Yee SS, O'Hara MH, Aggarwal C, Xin D, Shaked A, Gao M, Liu D, Borad MJ, Ramanathan RK, Carpenter EL, Ji A, de Beer MC, de Beer FC, Webb NR, Beatty GL. Hepatocytes direct the formation of a pro-metastatic niche in the liver. *Nature* 2019;567:249–252.
26. Knebel FH, Albuquerque RC, Massaro RR, Maria-Engler SS, Campa A. Dual effect of serum amyloid A on the invasiveness of glioma cells. *Mediat Inflamm* 2013; 2013:509089.
27. Sung H-J, Ahn J-M, Yoon Y-H, Rhim T-Y, Park C-S, Park J-Y, Lee S-Y, Kim J-W, Cho J-Y. Identification and validation of SAA as a potential lung cancer biomarker and its involvement in metastatic pathogenesis of lung cancer. *J Proteome Res* 2011;10:1383–1395.
28. Hiratsuka S, Watanabe A, Sakurai Y, Akashi-Takamura S, Ishibashi S, Miyake K, Shibuya M, Akira S, Aburatani H, Maru Y. The S100A8-serum amyloid A3-TLR4 paracrine cascade establishes a pre-metastatic phase. *Nat Cell Biol* 2008;10:1349–1355.
29. Niederau C, Backmerhoff F, Schumacher B, Niederau C. Inflammatory mediators and acute phase proteins in patients with Crohn's disease and ulcerative colitis. *Hepatogastroenterology* 1997;44:90–107.
30. Ishihara S, Tada Y, Kawashima K, Kataoka M, Sonoyama H, Yamashita N, Oka A, Kusunoki R, Fukuba N, Mishima Y, Oshima N, Moriyama I, Yuki T, Kinoshita Y. Serum amyloid A level correlated with endoscopic findings in patients with Crohn's disease—possible biomarker for evaluating mucosal healing. *Dig Liver Dis* 2018;50:553–558.
31. Yang F, de Villiers WJS, Lee EY, McClain CJ, Varilek GW. Increased nuclear factor-kappaB activation in colitis of interleukin-2-deficient mice. *J Lab Clin Med* 1999; 134:378–385.
32. de Villiers WJS, Varilek GW, de Beer FC, Guo J-T, Kindy MS. Increased serum amyloid A levels reflect colitis severity and precede amyloid formation in IL-2 knockout mice. *Cytokine* 2000;12:1337–1347.
33. Berg DJ, Davidson N, Kühn R, Müller W, Menon S, Holland G, Thompson-Snipes L, Leach MW, Rennick D. Enterocolitis and colon cancer in interleukin-10-deficient mice are associated with aberrant cytokine production and CD4(+) TH1-like responses. *J Clin Invest* 1996; 98:1010–1020.
34. Robertis MD, Massi E, Poeta ML, Carotti S, Morini S, Cecchetelli L, Signori E, Fazio VM. The AOM/DSS murine model for the study of colon carcinogenesis: from pathways to diagnosis and therapy studies. *J Carcinog* 2011;10:9.

35. Lee J-Y, Hall JA, Kroehling L, Wu L, Najar T, Nguyen HH, Lin W-Y, Yeung ST, Silva HM, Li D, Hine A, Loke P, Hudesman D, Martin JC, Kenigsberg E, Merad M, Khanna KM, Littman DR. Serum amyloid A proteins induce pathogenic Th17 cells and promote inflammatory disease. *Cell* 2019;180:79–91.e16.
36. Gouwy M, Buck M, Pörtner N, Opdenakker G, Proost P, Struyf S, Damme J. Serum amyloid A chemoattracts immature dendritic cells and indirectly provokes monocyte chemotaxis by induction of cooperating CC and CXC chemokines. *Eur J Immunol* 2015;45:101–112.
37. Sun L, Zhou H, Zhu Z, Yan Q, Wang L, Liang Q, Ye RD. Ex vivo and in vitro effect of serum amyloid A in the induction of macrophage M2 markers and efferocytosis of apoptotic neutrophils. *J Immunol* 2015;194:4891–4900.
38. Wang Y, Huang H, Sun R, Chen B, Han F, Li Q, Ni Y, Li X, Liu J, Mou X, Tu Y. Serum amyloid a induces M2b-like macrophage polarization during liver inflammation. *Oncotarget* 2017;8:109238–109246.
39. Buck MD, Gouwy M, Wang JM, Snick JV, Proost P, Struyf S, Damme JV. The cytokine-serum amyloid A-chemokine network. *Cytokine Growth Factor Rev* 2016;30:55–69.
40. Neurath MF. Cytokines in inflammatory bowel disease. *Nat Rev Immunol* 2014;14:329–342.
41. Lin H, Tan G, Liu Y, Lin S. The prognostic value of serum amyloid A in solid tumors: a meta-analysis. *Cancer Cell Int* 2019;19:62.
42. Bader JE, Enos RT, Velázquez KT, Carson MS, Nagarkatti M, Nagarkatti PS, Chatzistamou I, Davis JM, Carson JA, Robinson CM, Murphy EA. Macrophage depletion using clodronate liposomes decreases tumorigenesis and alters gut microbiota in the AOM/DSS mouse model of colon cancer. *Am J Physiol Gastrointest Liver Physiol* 2018;314:G22–G31.
43. Ather JL, Dienz O, Boyson JE, Anathy V, Amiel E, Poynter ME. Serum amyloid A3 is required for normal lung development and survival following influenza infection. *Sci Rep* 2018;8:16571.
44. Ebert R, Benisch P, Krug M, Zeck S, Meißner-Weigl J, Steinert A, Rauner M, Hofbauer L, Jakob F. Acute phase serum amyloid A induces proinflammatory cytokines and mineralization via toll-like receptor 4 in mesenchymal stem cells. *Stem Cell Res* 2015;15:231–239.
45. Reigstad CS, Lundén GÖ, Felin J, Bäckhed F. Regulation of serum amyloid A3 (SAA3) in mouse colonic epithelium and adipose tissue by the intestinal microbiota. *PLoS One* 2009;4:e5842.
46. Bábíčková J, Tóthová Ľ, Lengyelová E, Bartoňová A, Hodosy J, Gardlík R, Celec P. Sex differences in experimentally induced colitis in mice: a role for estrogens. *Inflammation* 2015;38:1996–2006.
47. Resta-Lenert S, Smitham J, Barrett KE. Epithelial dysfunction associated with the development of colitis in conventionally housed *mdr1a*^{-/-} mice. *Am J Physiol Gastrointest Liver Physiol* 2005;289:G153–G162.
48. Shah SC, Khalili H, Gower-Rousseau C, Olen O, Benchimol EI, Lynge E, Nielsen KR, Brassard P, Vutcovici M, Bitton A, Bernstein CN, Leddin D, Tamim H, Stefansson T, Loftus EV, Moum B, Tang W, Ng SC, Geary R, Sincic B, Bell S, Sands BE, Lakatos PL, Végh Z, Ott C, Kaplan GG, Burisch J, Colombel J-F. Sex-based differences in incidence of inflammatory bowel diseases—pooled analysis of population-based studies from Western countries. *Gastroenterology* 2018;155:1079–1089.e3.
49. Klein SL, Flanagan KL. Sex differences in immune responses. *Nat Rev Immunol* 2016;16:626–638.
50. Verdú EF, Deng Y, Bercik P, Collins SM. Modulatory effects of estrogen in two murine models of experimental colitis. *Am J Physiol Gastrointest Liver Physiol* 2002;283:G27–G36.
51. Soriano S, Moffet B, Wicker E, Villapol S. Serum amyloid A is expressed in the brain after traumatic brain injury in a sex-dependent manner. *Cell Mol Neurobiol* 2020;40:1199–1211.
52. Yu N, Zhang S, Lu J, Li Y, Yi X, Tang L, Su L, Ding Y. Serum amyloid A, an acute phase protein, stimulates proliferative and proinflammatory responses of keratinocytes. *Cell Prolif* 2016;50:e12320.
53. Yang R-Z, Lee M-J, Hu H, Pollin TI, Ryan AS, Nicklas BJ, Snitker S, Horenstein RB, Hull K, Goldberg NH, Goldberg AP, Shuldiner AR, Fried SK, Gong D-W. Acute-phase serum amyloid a: an inflammatory adipokine and potential link between obesity and its metabolic complications. *PLoS Med* 2006;3:e287.
54. Siegmund SV, Schlosser M, Schildberg FA, Seki E, Minicis SD, Uchinami H, Kuntzen C, Knolle PA, Strassburg CP, Schwabe RF. Serum amyloid A induces inflammation, proliferation and cell death in activated hepatic stellate cells. *PLoS One* 2016;11:e0150893.
55. de Beer MC, Webb NR, Wroblewski JM, Noffsinger VP, Rateri DL, Ji A, van der Westhuyzen DR, de Beer FC. Impact of serum amyloid A on high density lipoprotein composition and levels. *J Lipid Res* 2010;51:3117–3125.
56. Thaker AI, Shaker A, Rao MS, Ciorba MA. Modeling colitis-associated cancer with azoxymethane (AOM) and dextran sulfate sodium (DSS). *J Vis Exp* 2012;67:4100.
57. Schindelin J, Arganda-Carreras I, Frise E, Kaynig V, Longair M, Pietzsch T, Preibisch S, Rueden C, Saalfeld S, Schmid B, Tinevez J-Y, White DJ, Hartenstein V, Eliceiri K, Tomancak P, Cardona A. Fiji: an open-source platform for biological-image analysis. *Nat Methods* 2012;9:676–682.
58. Murthy SNS, Cooper HS, Shim H, Shah RS, Ibrahim SA, Sedergran DJ. Treatment of dextran sulfate sodium-induced murine colitis by intracolonic cyclosporin. *Dig Dis Sci* 1993;38:1722–1734.
59. Snider AJ, Bialkowska AB, Ghaleb AM, Yang VW, Obeid LM, Hannun YA. Murine model for colitis-associated cancer of the colon. In: Proetzel G, Wiles M, eds. *Mouse models for drug discovery*. New York: Humana Press, 2016:245–254.
60. Park A-M, Tsunoda I. Forensic luminol reaction for detecting fecal occult blood in experimental mice. *Biotechniques* 2018;65:227–230.
61. Erben U, Loddenkemper C, Doerfel K, Spieckermann S, Haller D, Heimesaat MM, Zeitz M, Siegmund B, Kühl AA.

A guide to histomorphological evaluation of intestinal inflammation in mouse models. *Int J Clin Exp Pathol* 2014;7:4557–4576.

62. Pham N-A, Morrison A, Schwock J, Aviel-Ronen S, Iakovlev V, Tsao M-S, Ho J, Hedley DW. Quantitative image analysis of immunohistochemical stains using a CMYK color model. *Diagn Pathol* 2007; 2:8.
63. Fuhrich DG, Lessey BA, Savaris RF. Comparison of HSCORE assessment of endometrial beta3 integrin subunit expression with digital HSCORE using computerized image analysis (ImageJ). *Anal Quant Cytopathol Histopathol* 2013;35:210–216.
64. Mustafa HN, Awdan SAE, Hegazy GA, Jaleel GAA. Prophylactic role of coenzyme Q10 and Cynara scolymus L on doxorubicin-induced toxicity in rats: biochemical and immunohistochemical study. *Indian J Pharmacol* 2015; 47:649–656.

Received February 23, 2021. Accepted June 21, 2021.

Correspondence

Address correspondence to: Willem J. S. de Villiers, MD, PhD, Stellenbosch

University, Admin B, Victoria Street, Stellenbosch, 7600, South Africa. e-mail: wimdv@sun.ac.za; fax: +27 21 808 3714

Acknowledgments

The authors thank Carla Fourie for assistance with the animal study, Manisha du Plessis for assistance with the immunohistochemical experiments, and Candice Snyders for assistance with the multiplex assay.

CRedit Authorship Contributions

Tanja Davis, PhD (Conceptualization: Equal; Formal analysis: Lead; Funding acquisition: Supporting; Investigation: Lead; Project administration: Lead; Validation: Lead; Visualization: Lead; Writing – original draft: Lead; Writing – review & editing: Equal)

Daleen Conradie, MSc (Investigation: Supporting; Writing – review & editing: Supporting)

Preetha Shridas, PhD (Resources: Supporting; Writing – review & editing: Equal)

Frederick de Beer, MD (Resources: Equal; Writing – review & editing: Equal)
Anna-Mart Engelbrecht, PhD (Funding acquisition: Equal; Resources: Equal; Supervision: Supporting; Writing – review & editing: Equal)

Willem JS de Villiers, MD, PhD (Conceptualization: Equal; Funding acquisition: Equal; Supervision: Lead; Writing – review & editing: Equal)

Conflicts of interest

The authors disclose no conflicts.

Funding

This work was supported financially by the South African Medical Research Council (A.-M.E.), the Cancer Association of South Africa (A.-M.E.), and National Research Foundation of South Africa grants 112018 (T.A.D.) and 118566 (A.-M.E.). The funding bodies had no role in the study design, collection, analyses, or interpretation of the data.